



## LJMU Research Online

Hulshof, HG, van Dijk, AP, Hopman, MTE, Heesakkers, H, George, KP, Oxborough, D and Thijssen, DHJ

**5-Year prognostic value of the right ventricular strain-area loop in patients with pulmonary hypertension.**

<http://researchonline.ljmu.ac.uk/id/eprint/13292/>

### Article

**Citation** (please note it is advisable to refer to the publisher's version if you intend to cite from this work)

**Hulshof, HG, van Dijk, AP, Hopman, MTE, Heesakkers, H, George, KP, Oxborough, D and Thijssen, DHJ (2020) 5-Year prognostic value of the right ventricular strain-area loop in patients with pulmonary hypertension. *European Heart Journal Cardiovascular Imaging*. 22 (2). pp. 188-195. ISSN**

LJMU has developed [LJMU Research Online](http://researchonline.ljmu.ac.uk/) for users to access the research output of the University more effectively. Copyright © and Moral Rights for the papers on this site are retained by the individual authors and/or other copyright owners. Users may download and/or print one copy of any article(s) in LJMU Research Online to facilitate their private study or for non-commercial research. You may not engage in further distribution of the material or use it for any profit-making activities or any commercial gain.

The version presented here may differ from the published version or from the version of the record. Please see the repository URL above for details on accessing the published version and note that access may require a subscription.

For more information please contact [researchonline@ljmu.ac.uk](mailto:researchonline@ljmu.ac.uk)

<http://researchonline.ljmu.ac.uk/>

1                   **5-YEAR PROGNOSTIC VALUE OF THE RIGHT**  
2                   **VENTRICULAR STRAIN-AREA LOOP IN PATIENTS WITH**  
3                   **PULMONARY HYPERTENSION**

4  
5  
6                   HUGO G. HULSHOF<sup>1</sup>

7                   ARIE P. VAN DIJK<sup>2</sup>

8                   MARIA T.E. HOPMAN<sup>1</sup>

9                   HIDDE HEESAKKERS<sup>1</sup>

10                  KEITH P. GEORGE<sup>3</sup>

11                  DAVID L. OXBOROUGH<sup>3\*</sup>

12                  DICK H.J. THIJSEN<sup>1,3\*</sup>

13                  \* = BOTH AUTHORS CONTRIBUTED EQUALLY

14  
15  
16                  <sup>1</sup>Research Institute for Health Sciences, Department of Physiology, Radboud University  
17                                  Medical Center, Nijmegen, The Netherlands

18                  <sup>2</sup>Research Institute for Health Sciences, Department of Cardiology, Radboud University  
19                                  Medical Center, Nijmegen, The Netherlands

20                  <sup>3</sup>Research Institute for Sport and Exercise Sciences, Liverpool John Moores University,  
21                                  Liverpool, United Kingdom'

22  
23  
24  
25                  **Short title:** Strain-area loop in Pulmonary Hypertension

26  
27  
28                  **Author for correspondence:** Prof. Dick H.J. Thijssen, Department of Physiology  
29                  Radboud University Medical Center, Philips van Leijdenlaan 15, 6525 EX, Nijmegen, The  
30                  Netherlands, Email: dick.thijssen@radboudumc.nl, Tel: (+31) 24 361 4222, Fax: (+31) 24

31                                  366 8340

32 **ABSTRACT**

33 **Aims.** Patients with pre-capillary pulmonary hypertension (PH) show poor survival, often  
34 related to right ventricular (RV) dysfunction. In this study we assessed the 5-year prognostic  
35 value of a novel echocardiographic measure that examines RV function through the temporal  
36 relation between RV strain ( $\epsilon$ ) and area (i.e. RV  $\epsilon$ -area loop) for all-cause mortality in PH  
37 patients.

38 **Methods and results.** Echocardiographic assessments were performed in 143 PH patients  
39 (confirmed by right heart catheterization). Transthoracic echocardiography was utilised to  
40 assess RV  $\epsilon$ -area loop. Using ROC-derived cut-off values, we stratified patients in low- *versus*  
41 high-risk groups for all-cause mortality. Kaplan-Meier survival curves and uni-/multivariable  
42 cox-regression models were used to assess RV  $\epsilon$ -area loop's prognostic value (independent of  
43 established predictors: age, sex, NT-proBNP, 6-minute walking distance).

44 During follow-up 45 (31%) patients died, who demonstrated lower systolic slope, peak  $\epsilon$ , and  
45 late diastolic slope (all  $P < 0.05$ ) at baseline. Univariate cox-regression analyses identified early  
46 systolic slope, systolic slope, peak  $\epsilon$ , early diastolic uncoupling and early/late diastolic slope to  
47 predict all-cause mortality (all  $P < 0.05$ ), whilst peak  $\epsilon$  possessed independent prognostic value  
48 ( $P < 0.05$ ). High RV loop-score (i.e. based on number of abnormal characteristics) showed  
49 poorer survival compared to low RV loop-score (Kaplan-Meier:  $P < 0.01$ ). RV loop-score  
50 improved risk stratification in high-risk patients when added to established predictors.

51 **Conclusion.** Our data demonstrates the potential for RV  $\epsilon$ -area loops to independently predict  
52 all-cause mortality in patients with pre-capillary PH. The non-invasive nature and simplicity of  
53 measuring the RV  $\epsilon$ -area loop, support the potential clinical relevance of (repeated)  
54 echocardiography assessment of PH patients.

55

56 **KEYWORDS:** pulmonary hypertension; prognostic value; echocardiography, right  
57 ventricular function; ultrasound

58 **INTRODUCTION**

59 Pulmonary hypertension (PH) is a progressive pulmonary vascular disease, which is associated  
60 with a poor 5-year survival-rate.(1) The primary cause of death relates to deterioration of right  
61 ventricular (RV) function, caused by the inability of the RV to overcome the increased  
62 afterload.(2) Approximately 44% of all deaths in patients with PH is caused by RV failure or  
63 sudden death.(3) Despite the inherent connection between PH-related death and RV function,  
64 current risk assessment guidelines only includes cardiac index (derived by invasive right heart  
65 catheterization (RHC)) and right atrial (RA) area as variables of RV function.(4) Given the  
66 invasiveness of RHC, associated risks/complications and inability for repeated measurements,  
67 alternative non-invasive measures of RV function may be more suitable in PH.

68

69 Although right heart echocardiography is advised in suspicion of PH and/or during follow-up  
70 of patients with PH, it possesses inferior prognostic value compared to other clinical measures  
71 (i.e. 6-minute walking distance (6M-WD), NT-proBNP) and RHC.(4) RV longitudinal  $\epsilon$  (a  
72 relatively novel echocardiographic derived indices) possesses independent prognostic value for  
73 PH-related events and all-cause mortality(5) and has been shown to be a stronger predictor than  
74 tricuspid annular plane excursion (TAPSE) (6) in patients with pre-capillary PH.

75

76 Recently, we introduced the RV  $\epsilon$ -area loop, which reflects the change of RV longitudinal  $\epsilon$   
77 across the cardiac cycle and is linked to the change in RV area.(7, 8) Simultaneous assessment  
78 of RV longitudinal  $\epsilon$  and area provides novel insight into the contribution of RV longitudinal  
79 contraction and relaxation to area change. Interestingly, we found that the slope of the systolic  
80  $\epsilon$ -area relation is strongly related to pulmonary vascular resistance.(8) This raises questions  
81 about the potential prognostic value of the RV  $\epsilon$ -area loop for future PH-related events and (all-  
82 cause) mortality.

83 The primary aim of this study was to examine the prognostic value of characteristics of the RV  
84  $\epsilon$ -area loop for future all-cause mortality in patients with pre-capillary PH across a 5-year  
85 follow-up. We hypothesize that characteristics of the RV  $\epsilon$ -area loop (e.g. slope of the systolic  
86  $\epsilon$ -area relation) possesses predictive value for all-cause mortality in patients with pre-capillary  
87 PH, independent from currently known predictors (i.e., age, sex, 6M-WD, NT-proBNP).

88

## 89 **METHODS**

### 90 *Ethics approval*

91 Ethics approval was obtained from the Radboud University Medical Center ethics committee  
92 to perform the proposed work (reference number 2015-1832). This study was registered at the  
93 Netherlands Trial Register (NTR5230) and conforms to the standards set by the latest revision  
94 of the Declaration of Helsinki.

95

### 96 *Study population*

97 We included 177 patients with pre-capillary PH, confirmed by RHC, who underwent  
98 transthoracic echocardiography at the department of Cardiology of the Radboud University  
99 Medical Center (Nijmegen) between June 2003 and June 2017. Patients with multifactorial PH  
100 were included when pre-capillary PH was confirmed and PH-modifying therapy was  
101 prescribed. Due to inadequate 2D image quality for RV longitudinal  $\epsilon$  analysis, 44 patients were  
102 excluded, resulting in a final cohort of 143 patients. Additional information regarding the  
103 included population can be found in Table 1.

104

### 105 *Experimental design*

106 To address our aims, we retrospectively collected data on patient characteristics, PH-modifying  
107 therapy, 6M-WD and NT-proBNP at the time of echocardiographic assessment. Survival status

108 of patients was retrieved from the Dutch population register at 21-01-2019, resulting in median  
109 follow-up of 60[interquartile range: 45-60] months while 91 patients fulfilled the maximal  
110 follow-up of 5-years.

111

### 112 *Echocardiographic assessment*

113 Echocardiographic data was obtained by experienced sonographers using ultrasounds machines  
114 of the Vivid series (GE Healthcare, Horton, Norway). Data were stored in raw DICOM format  
115 in a password-protected archive of the department of Cardiology of the Radboud University  
116 Medical Center. Data were retrieved for subsequent analysis by a single experienced researcher  
117 using commercially available software (EchoPac version 113.05, GE Healthcare, Horten,  
118 Norway). This researcher was blinded for the outcome during follow-up.

119

### 120 *Conventional Echocardiographic Assessment*

121 Conventional echocardiographic indices were obtained in accordance with ASE Guidelines for  
122 echocardiographic assessment of the right heart.(9) RV end diastolic area (RVEDA) and RV  
123 end systolic area (RVESA) were measured during the same cardiac cycle from a modified apical  
124 4 chamber orientation. RVFAC was calculated as  $((RVEDA-RVESA)/RVEDA)*100$ . TAPSE  
125 was determined using an M-Mode image for measuring the displacement of the tricuspid  
126 annulus.

127

### 128 *2D Myocardial Speckle Tracking*

129 A modified apical 4-chamber view, with a frame-rate of at least 40 frames per second, was used  
130 to assess simultaneous RV longitudinal  $\epsilon$  and area. Images were optimized to ensure adequate  
131 endocardial delineation using gain, compression and reject. A region of interest (ROI) was  
132 drawn from the basal free to the basal septal wall enclosing the entire myocardium. Automatic

133 analysis divided this ROI in six segments, the average of these segments (i.e. RV global  
134 longitudinal  $\epsilon$ ) was used in subsequent analysis.(7) RV global longitudinal  $\epsilon$  instead of RV free  
135 wall  $\epsilon$  was used to ensure the inclusion of changes in RV function due to ventricular  
136 dyssynchrony as present in patients with pre-capillary PH.(10)

137

### 138 *RV $\epsilon$ -area loops*

139 Temporal RV longitudinal  $\epsilon$  values were exported to a spreadsheet (Excel, Microsoft Corp,  
140 Washington, US). To correct for differences in HR between subjects and length of the systolic  
141 and diastolic part of cardiac cycle, the temporal RV longitudinal  $\epsilon$  values were divided in 300  
142 points for systole and 300 points for diastole by cubic spline interpolation. For both systole and  
143 diastole the 300  $\epsilon$  values were then split into 5% increments of the cardiac cycle providing 10  
144 points in systole and 10 points in diastole. Concomitant time points, derived by tracing the  
145 echocardiography derived ECG signal, of the  $\epsilon$  values were used in the same image and cardiac  
146 cycle to trace RV monoplane areas. For each patient, an RV  $\epsilon$ -area loop was created.

147

148 The RV  $\epsilon$ -area loops were assessed by 1) the early systolic  $\epsilon$ -area relation (ESslope), 2) linear  
149 slope of  $\epsilon$ -area relation during systole (Sslope), 3) end systolic peak  $\epsilon$  (peak  $\epsilon$ ), 4) diastolic  
150 uncoupling (i.e. mean difference between systolic vs diastolic  $\epsilon$  contribution to area change)  
151 during early filling (UNCOUP\_ED), 5) diastolic uncoupling during late diastole  
152 (UNCOUP\_LD), 6) diastolic uncoupling during the entire cardiac cycle (UNCOUP), 7) the  
153 early diastolic  $\epsilon$ -area relation (EDslope) and 8) the late diastolic  $\epsilon$ -area relation (LDslope) as  
154 presented in Figure 1. Based on our extensive pilot work (7, 8, 11) we adopted either a linear  
155 regression (i.e. Sslope) or a second order polynomial (i.e. ESslope, UNCOUP\_ED,  
156 UNCOUP\_LD UNCOUP, EDslope and LDslope) approach for data analysis as these models  
157 provide the best fit. Specifically, ESslope was calculated as the contribution of RV longitudinal

158  $\epsilon$  to the first 5% of area change. The Sslope was derived as the gradient over the systolic phase  
159 of the RV  $\epsilon$ -area loop. Longitudinal peak  $\epsilon$  was derived as the raw peak  $\epsilon$  value from the RV  
160 global longitudinal  $\epsilon$  data. UNCOUP\_ED, UNCOUP\_LD and UNCOUP were calculated as an  
161 normalized estimation of the area between the systolic and diastolic strain-area curves. For this  
162 purpose, systolic and diastolic  $\epsilon$  values were calculated at each % increment of EDA.  
163 Subsequently, the difference between diastolic and systolic  $\epsilon$  at each % of EDA was calculated.  
164 Based on individual RVFAC the working range of the ventricle was determined, after which  
165 UNCOUP\_ED, UNCOUP\_LD and UNCOUP were calculated as the mean of the differences at  
166 the lowest 2/3 of EDA's, at the highest 1/3 of EDA's and over the entire working range  
167 respectively. EDslope and LDslope were calculated as the contribution of RV longitudinal  $\epsilon$  to  
168 the first and last 5% of area change respectively. In addition, we calculated the Intra-class  
169 correlation (ICC) for intra-rater variability for all loop characteristics in a healthy population  
170 (n=7), with exception of UNCOUP\_LD, we retrieved good to excellent ICC (supplementary  
171 Table 1)

172

### 173 *Statistical analysis*

174 Continuous variables were expressed as mean $\pm$ SD in case of normal distribution. Normality of  
175 data distribution was examined using a Kolmogorov-Smirnov test. In case of non-Gaussian  
176 distribution, log-transformation was applied and data was presented as median[interquartile  
177 range]. Categorical variables were expressed as percentage. Patients lost to follow-up were  
178 censored at the time of last available follow-up.

179

180 *Cut-off values for risk stratification.* Based on the optimal combination of sensitivity and  
181 specificity, derived from ROC-analyses at 5-year follow-up, cut-off values for all  
182 echocardiographic derived parameters were obtained (Supplementary Table 2). Based on this



183 cut-off value, patients were divided into low *versus* high risk for all-cause mortality. Cut-off  
184 values for established predictors (6M-WD, NT-proBNP, RA area) for low *versus* high risk group  
185 were based on current guidelines.(4)

186

187 *Survival analysis.* Kaplan-Meier survival curves were constructed to assess discriminative  
188 capacity of the RV  $\epsilon$ -area loop characteristics. Univariate cox proportional hazard ratios were  
189 determined to assess the predictive value of RV  $\epsilon$ -area loop characteristics for all-cause  
190 mortality. Subsequently, significant univariate predictors were fitted into multivariable models  
191 to determine their independent predictive value compared to the reference model (consisting of  
192 age, sex, 6M-WD, and NT-proBNP). Finally, we calculated a combined RV loop-score based  
193 on the RV  $\epsilon$ -area loop characteristics with predictive value after univariate cox regression  
194 analyses (n=6, Table 3), combining the risk stratifications of the individual characteristics. The  
195 RV loop-score was ranged between 0 and 6 (i.e. 1 point for each characteristic in the high-risk  
196 category), categorising patients with ‘low score’ (RV loop-score of 0-3) *versus* ‘high score’  
197 (RV loop-score of 4-6). First, we examined the Kaplan-Meier curve based on the RV loop-  
198 score. Secondly, we examined if the RV loop-score improved risk stratification based on the  
199 2015 ESC/ERS guidelines for diagnosis and treatment of PH (including NT-proBNP, RA area  
200 and 6M-WD) that is clinically used to categorise PH patients into low, intermediate and high  
201 risk.

202

## 203 **RESULTS**

204 Of the 143 patients, 117 were diagnosed with WHO class 1 PH, consisting of 95 patients with  
205 (idiopathic) pulmonary artery hypertension (PAH) and 22 with multifactorial PH. The  
206 remaining 26 patients were diagnosed with WHO class IV PH, i.e. Chronic Trombo-Embolic  
207 PH (CTEPH).

208 *Follow-up.* After a median follow-up period of 60 [45-60] months, 45 out of 143 patients died  
209 (5-year survival: 69%). Patients who died were older, predominantly male sex, had a higher  
210 NT-proBNP level, showed larger RVEDA and RVESA, and lower 6M-WD and RVFAC at  
211 baseline (all  $P < 0.05$ , Table 2). A marked rightward shift in the RV  $\epsilon$ -area loop was visible at  
212 baseline between surviving and deceased patients (Figure 2). A significantly lower Sslope,  
213 EDslope, and peak  $\epsilon$  was found in deceased *versus* surviving patients after 5-years follow-up  
214 (all  $P < 0.05$ , Table 2). Kaplan-Meier survival analysis revealed significant differences in  
215 survival when patients were categorised based on ESslope, Sslope, Peak  $\epsilon$ , EDslope and  
216 LDslope of the RV  $\epsilon$ -area loop (Figure 3).

217

218 *Uni- and multivariate Cox regression.* Univariate cox regression analysis revealed age, sex,  
219 NT-proBNP, 6M-WD, RVEDA, RVESA, RVFAC, TAPSE and RV  $\epsilon$ -area loop characteristics  
220 (ESslope, Sslope, peak  $\epsilon$ , Uncoup\_ED, ESslope and LDslope) as univariate predictors for 5-  
221 year all-cause mortality (Table 3). Multivariable models revealed that RVESA ( $>16.9 \text{ cm}^2$ ),  
222 RVFAC ( $<25.55\%$ ) and peak  $\epsilon$  ( $>-14.45\%$ ) remained significant predictors when added to the  
223 reference model (Table 4).

224

225 *RV loop-score.* Kaplan-Meier survival curves revealed significant differences in 5-year survival  
226 between 'low' and 'high' RV loop-scores (Figure 4A). Hazard Ratio showed a 3.182 [1.768-  
227 5.726] times higher risk for all-cause mortality in those with a 'high' RV loop-score compared  
228 to 'low' loop-score. More importantly, the RV loop-score improved risk classification  
229 following the 2015 ESC/ERS guidelines (Figure 4B), with high risk individuals with 'low' RV  
230 loop-scores showing significantly better survival than high risk patients with an 'high' RV loop-  
231 score (Kaplan-Meier:  $P=0.02$ , Figure 4C). The RV loop-score did not significantly improve  
232 classification of patients at low ( $P=0.83$ ) and intermediate ( $P=0.91$ ) risk.

233 **DISCUSSION**

234 The purpose of this study was to examine the 5-year prognostic value of RV  $\epsilon$ -area loop  
235 characteristics for all-cause mortality in patients with pre-capillary PH. We present the  
236 following findings: 1) A markedly different RV  $\epsilon$ -area loop is present in PH patients who died  
237 across 5-year follow-up compared to surviving patients, 2) RV  $\epsilon$ -area loop characteristics show  
238 significant prognostic value for 5-yr all-cause mortality in PH patients, with RV longitudinal  
239 peak  $\epsilon$  possessing independent prognostic value, 3) The RV loop-score, i.e. reflecting the  
240 number of 'abnormal' loop characteristics, successfully predicts 5-yr all-cause mortality in PH  
241 patients, but also improves risk stratification in the high risk population. Taken together, our  
242 findings suggest the RV  $\epsilon$ -area loop predicts all-cause mortality in patients with pre-capillary  
243 PH and may reclassify some patients from the high-risk group to an intermediate-risk group.  
244 The non-invasive nature and relative simplicity of measuring the RV  $\epsilon$ -area loop, support the  
245 potential clinical relevance of echocardiography for (repeated) assessment of PH patients.

246

247 The marked shift between the RV  $\epsilon$ -area loop of the surviving and deceased patients suggests  
248 the presence of a (further) impairment in RV function at the time of echocardiographic  
249 assessment in the deceased patients. The lower peak  $\epsilon$  and flatter systolic  $\epsilon$ -area slopes may be  
250 related to an impaired RV systolic function, presented by the smaller deformation (i.e.  $\epsilon$ ) of the  
251 ventricular wall for each  $\text{cm}^2$  change in area in the deceased patients compared to those who  
252 survived. These adaptations may be the consequence of the RV being exposed to increased  
253 afterload(12). However, no differences in mean pulmonary artery pressure or pulmonic vascular  
254 resistance were present between both groups. Possibly, different RV  $\epsilon$ -area loop characteristics  
255 between groups may relate to the presence of maladaptation in the deceased group (i.e. dilation  
256 of ventricles).(13) Similarly to the impaired systolic function, the lower diastolic  $\epsilon$ -area slopes  
257 suggest that although RV area is increasing eventually, less contribution from longitudinal

258 strain is present during early relaxation in deceased patients compared to those who survived.  
259 In line with our observation, others have shown increased isovolumetric relaxation times in  
260 patients with PH(14), indicating poor myocardial relaxation(15) and diminished ventricular  
261 compliance. Taken together, both systolic and diastolic RV  $\epsilon$ -area loop characteristics seem  
262 impaired in PH patients at higher risk for all-cause mortality across a 5-year follow-up.

263

264 Despite the growing consensus of the importance of RV function in patients with pre-capillary  
265 PH,(16) current guidelines only include RA area, presence of pericardial effusion and through  
266 RHC obtained cardiac index to predict mortality.(4) Interestingly, our study found no  
267 prognostic value of RA area, whilst measures the novel RV  $\epsilon$ -area loop possessed predictive  
268 capacity. To further support the relevance of echocardiography, RVESA (<16.9), RVFAC  
269 (<25.5%) and RV longitudinal peak  $\epsilon$  (>-14.45)) possessed independent predictive value for  
270 all-cause mortality (Table 4). These results confirm findings of previous studies assessing the  
271 prognostic value of echocardiography in patients with pre-capillary PH.(17, 18) It is important  
272 to emphasize that we used ROC-analyses to determine the threshold for low *versus* high risk.  
273 A potential limitation of this approach is that these thresholds cannot be simply applied to other  
274 data sets. This highlights the importance of defining reference values for echocardiographic  
275 derived indices of RV function.

276

277 A key observation in our study was the prognostic value of both systolic and diastolic RV  $\epsilon$ -  
278 area loop characteristics. Traditionally, markers of RV function only include RV systolic  
279 function. In a recent study, it was demonstrated that deterioration of RV diastolic function may  
280 precede deterioration of RV systolic function in patients with pre-capillary PH.(14) This  
281 suggests that the processes of diastolic and systolic dysfunction represent linked, but possibly  
282 independent impact. In support of this view, we found only low-to-moderate correlations

283 ( $r^2=0.07-0.45$ ) between indices of systolic function (ESslope, Sslope) and diastolic function  
284 (EDslope, LDslope) of the RV  $\epsilon$ -area loop. This data highlights that the combined temporal  
285 data on the relative contribution of strain to area change during both systole and diastole, and  
286 the association between systolic and diastolic function, provide in depth insights in ventricular  
287 function compared to single peak value based assessments such as peak strain or RVFAC.  
288 The dynamic temporal data acquired within the strain-area loop therefore increases its  
289 predictive value over functional measures at a single point during the cardiac cycle.

290

291 Presence of predictive value of the individual indices (including both systolic and diastolic RV  
292 function), and absence of strong relations amongst the 6 individual RV  $\epsilon$ -area loop  
293 characteristics ( $r^2=0.001-0.47$ ), support the potential value of calculating a multi-parameter  
294 value such as an RV loop-score. Whilst the RV loop-score showed strong and significant  
295 prognostic value, adding the RV loop-score to the clinically used, 2015 ESC/ERS guidelines  
296 improved risk stratification for the high-risk population. More specifically, high risk patients  
297 with a low RV loop-score showed a significantly better 5-year survival than those with a high  
298 RV loop-score. Effectively, the high-risk patients with low RV loop-scores were reclassified as  
299 moderate risk, given their similar survival curves (Figure 4C). This may be explained by the  
300 absence of echocardiographic RV function indices in the 2015 ESC/ERS risk stratification  
301 guidelines. Since deterioration of RV function remains the main cause of death in patients with  
302 pre-capillary PH,(16) stratification of PH patients may be improved by including characteristics  
303 of RV function.

304

305 *Clinical implications.* The prognostic capacity, but especially the ability of the RV  $\epsilon$ -area loop  
306 to reclassify high-risk patients to intermediate-risk, has potential clinical importance. Following  
307 the 2015 ESC/ERS guidelines, predicting all-cause mortality and classifying PH patients

308 importantly dictates clinical decision making related to (non)pharmaceutical therapy.  
309 Specifically, excessive physical activity is not recommended in high-risk patients, whilst an  
310 increasing amount of follow-up visits and more aggressive PH-modifying therapy strategy is  
311 advised for high-risk patients. Successfully reclassifying the high-risk to intermediate-risk, i.e.  
312 51% of our population, will therefore impact treatment (and lower associated costs and risks  
313 for complications/side-effects). Finally, the ability for repeated assessment of RV function  
314 enables evaluation of disease progress and efficacy of (non)pharmaceutical therapy.

315

316 *Limitations.* Although all patients had pre-capillary PH, different etiology was present. Whilst  
317 our sample size is sufficiently powered to identify predictors for all-cause mortality in PH, it  
318 does not allow for sub-analyses related to the various aetiology of PH. Another limitation is  
319 that some patients (n=54) received PH-modifying therapy prior to inclusion. A sub-analysis  
320 revealed no differences in the RV  $\epsilon$ -area loop characteristic at the time of inclusion between  
321 those with and without PH-modifying therapy prior to inclusion (supplementary table 3).  
322 Moreover, patients with PH-modifying therapy at time of inclusion, typically started this within  
323 weeks prior to inclusion, whilst the majority started PH-modifying therapy within 1 week after  
324 the day of inclusion. Therefore, this short time-frame wherein all participants started PH-  
325 modifying therapy unlikely affected the main outcomes of our study. Finally, the current  
326 method to assess the  $\epsilon$ -volume loops and their characteristics is currently only partially  
327 automated and thus time-consuming. Automated self-learning analysis protocols should be  
328 created prior to clinical implementation. In response to the time-consuming nature of the current  
329 loops analysis we have analysed a simplified parameter, here called the endsystolic-enddiastolic  
330  $\epsilon$ -area slope (ESEDslope), which provides the systolic slope based on individual measures of  
331 just RVEDA, RVESA and Peak  $\epsilon$ . Similar too the Sslope significant differences were found for  
332 ESEDslope between groups (Alive vs. Deceased;  $1.80 \pm 0.74$  vs.  $1.49 \pm 0.55$ ;  $P=0.01$ ) and a

333 significant HR (2.084 [1.140-3.811]; P=0.02) using a univariate analysis. In line with the slope  
334 significance disappeared when ESEDslope was added to the reference model (HR: 1.449  
335 [0.663-3.168]; P=0.35). This suggests that the combination of characteristics for the loop may  
336 outperform individual, simplified measures. This outcome supports the use of multiple  
337 measures from the  $\epsilon$ -area loop in predictive analysis.

338

339 In conclusion, our data demonstrate a distinct RV  $\epsilon$ -area loop in PH patients who deceased  
340 across a 5-yr follow-up since diagnosis compared to those who survived. Several RV  $\epsilon$ -area  
341 loop characteristics predict 5-yr all-cause mortality, with RV peak longitudinal  $\epsilon$  demonstrating  
342 independent prognostic value. More importantly, combining these RV  $\epsilon$ -area loop  
343 characteristics into a RV loop-score successfully stratified PH patients into high *versus* low risk  
344 for all-cause mortality, and improved risk stratification of the ‘high risk’ patients when added  
345 to the current (guidelines-based) risk assessment model. These results support the clinical  
346 potential of echocardiography-based assessment of the RV  $\epsilon$ -area loop for risk stratification and  
347 survival-analyses in patients with pre-capillary PH. Future studies are warranted to further  
348 explore its potential use, especially in the context of repeated assessment of echocardiography  
349 to monitor progression and adjust treatment to optimise care for this vulnerable group of  
350 patients.

351

## 352 **Acknowledgements**

353 None

354

## 355 **Sources of Funding**

356 This study was supported by a junior researcher grant from the Radboud Institute for Health  
357 Sciences.

358 **Disclosures**

359 Dr. van Dijk reports grants and personal fees from Actelion, outside the submitted work; The

360 other authors reported nothing to disclose.



361 **REFERENCES**

- 362 1. Gall H, Felix JF, Schneck FK, Milger K, Sommer N, Voswinckel R, et al. The Giessen  
363 Pulmonary Hypertension Registry: Survival in pulmonary hypertension subgroups. *J Heart*  
364 *Lung Transplant*. 2017;36(9):957-67.
- 365 2. Voelkel NF, Quaipe RA, Leinwand LA, Barst RJ, McGoon MD, Meldrum DR, et al.  
366 Right ventricular function and failure: report of a National Heart, Lung, and Blood Institute  
367 working group on cellular and molecular mechanisms of right heart failure. *Circulation*.  
368 2006;114(17):1883-91.
- 369 3. Tonelli AR, Arelli V, Minai OA, Newman J, Bair N, Heresi GA, et al. Causes and  
370 circumstances of death in pulmonary arterial hypertension. *Am J Respir Crit Care Med*.  
371 2013;188(3):365-9.
- 372 4. Galie N, Humbert M, Vachiery JL, Gibbs S, Lang I, Torbicki A, et al. 2015 ESC/ERS  
373 Guidelines for the diagnosis and treatment of pulmonary hypertension: The Joint Task Force  
374 for the Diagnosis and Treatment of Pulmonary Hypertension of the European Society of  
375 Cardiology (ESC) and the European Respiratory Society (ERS): Endorsed by: Association for  
376 European Paediatric and Congenital Cardiology (AEPC), International Society for Heart and  
377 Lung Transplantation (ISHLT). *Eur Heart J*. 2016;37(1):67-119.
- 378 5. Hulshof HG, Eijvogels TMH, Kleinnibbelink G, van Dijk AP, George KP,  
379 Oxborough DL, et al. Prognostic value of right ventricular longitudinal strain in patients with  
380 pulmonary hypertension: a systematic review and meta-analysis. *Eur Heart J Cardiovasc*  
381 *Imaging*. 2018.
- 382 6. Shukla M, Park JH, Thomas JD, Delgado V, Bax JJ, Kane GC, et al. Prognostic Value  
383 of Right Ventricular Strain Using Speckle-Tracking Echocardiography in Pulmonary  
384 Hypertension: A Systematic Review and Meta-analysis. *Can J Cardiol*. 2018;34(8):1069-78.
- 385 7. Oxborough D, Heemels A, Somauroo J, McClean G, Mistry P, Lord R, et al. Left and  
386 right ventricular longitudinal strain-volume/area relationships in elite athletes. *Int J*  
387 *Cardiovasc Imaging*. 2016;32(8):1199-211.
- 388 8. Hulshof HG, van Dijk AP, George KP, Merkus D, Stam K, van Duin RW, et al.  
389 Echocardiographic-Derived Strain-Area Loop of the Right Ventricle is Related to Pulmonary  
390 Vascular Resistance in Pulmonary Arterial Hypertension. *JACC Cardiovasc Imaging*.  
391 2017;10(10 Pt B):1286-8.
- 392 9. Rudski LG, Lai WW, Afilalo J, Hua L, Handschumacher MD, Chandrasekaran K, et  
393 al. Guidelines for the echocardiographic assessment of the right heart in adults: a report from  
394 the American Society of Echocardiography endorsed by the European Association of  
395 Echocardiography, a registered branch of the European Society of Cardiology, and the  
396 Canadian Society of Echocardiography. *J Am Soc Echocardiogr*. 2010;23(7):685-713; quiz  
397 86-8.
- 398 10. Schiller NB, Singh S. RV Dyssynchrony by Speckle Tracking Strain in Pulmonary  
399 Arterial Hypertension: Will This Outcome Variable Take Root? *JACC Cardiovasc Imaging*.  
400 2015;8(6):653-5.
- 401 11. Hulshof HG, van Dijk AP, George KP, Hopman MTE, Thijssen DHJ, Oxborough DL.  
402 Exploratory assessment of left ventricular strain-volume loops in severe aortic valve diseases.  
403 *J Physiol*. 2017;595(12):3961-71.
- 404 12. Brown SB, Raina A, Katz D, Szerlip M, Wiegers SE, Forfia PR. Longitudinal  
405 shortening accounts for the majority of right ventricular contraction and improves after  
406 pulmonary vasodilator therapy in normal subjects and patients with pulmonary arterial  
407 hypertension. *Chest*. 2011;140(1):27-33.

- 408 13. Buckberg G, Hoffman JI. Right ventricular architecture responsible for mechanical  
409 performance: unifying role of ventricular septum. *J Thorac Cardiovasc Surg.*  
410 2014;148(6):3166-71 e1-4.
- 411 14. Murch SD, La Gerche A, Roberts TJ, Prior DL, MacIsaac AI, Burns AT. Abnormal  
412 right ventricular relaxation in pulmonary hypertension. *Pulm Circ.* 2015;5(2):370-5.
- 413 15. Grapsa J, Dawson D, Nihoyannopoulos P. Assessment of right ventricular structure  
414 and function in pulmonary hypertension. *J Cardiovasc Ultrasound.* 2011;19(3):115-25.
- 415 16. Vonk Noordegraaf A, Galie N. The role of the right ventricle in pulmonary arterial  
416 hypertension. *Eur Respir Rev.* 2011;20(122):243-53.
- 417 17. Haeck ML, Scherptong RW, Marsan NA, Holman ER, Schalij MJ, Bax JJ, et al.  
418 Prognostic value of right ventricular longitudinal peak systolic strain in patients with  
419 pulmonary hypertension. *Circ Cardiovasc Imaging.* 2012;5(5):628-36.
- 420 18. Fine NM, Chen L, Bastiansen PM, Frantz RP, Pellikka PA, Oh JK, et al. Outcome  
421 prediction by quantitative right ventricular function assessment in 575 subjects evaluated for  
422 pulmonary hypertension. *Circ Cardiovasc Imaging.* 2013;6(5):711-21.
- 423

424

425 **TABLE 1** – Population characteristics of the included patients with pre-capillary PH.

	PH-patients (n=143)			
Age (y)	61±16			
Female (%)	100 (70%)			
Height(cm)	169±9			
Weight (Kg)	73±15			
BSA (m <sup>2</sup> )	1.82±0.19			
BMI (kg/m <sup>2</sup> )	26.0±4.9			
<b>Therapy at time of ultrasound</b>				
Treatment Naive	89 (62%)			
Single Therapy	24 (17%)			
Double Therapy	26 (18%)			
Triple Therapy	4 (3%)			
<b>Aetiology</b>				
PAH	55 (38%)			
<i>IPAH</i>	40 (28%)			
<i>CTEPH</i>	26 (18%)			
<i>Multifactorial</i>	22 (15%)			
<b>Risk factors</b>				
	Yes	No	Unknown	Former
Hypertensive	41	39	63	
Dyslipidemia	21	41	81	
Diabetes Mellitus	15	52	76	
Smoker	16	41	27	59
Familiar history	34	41	68	

426 PH=Pulmonary Hypertension; BSA=Body Surface Area; BMI=Body Mass Index;

427 PAH=Pulmonary Arterial Hypertension; IPAH=Idiopathic Pulmonary Arterial Hypertension;

428 CTEPH=Chronic Thrombo-Embollic Pulmonary Hypertension.

429

430 **TABLE 2** – Population characteristics of the surviving and deceased patients after 5 years  
 431 follow-up.

	<b>60 [45-60] months follow up</b>		
	Alive (n=98)	Deceased (n=45)	P-Value
<b><i>Demographics</i></b>			
Age (y)	59±17	64±14	0.08
Height(m)	167±0.09	169±0.09	0.27
Weight (kg)	73±15	74±14	0.73
BSA (m <sup>2</sup> )	1.81±0.19	1.84±0.18	0.43
BMI (kg/m <sup>2</sup> )	26.0±4.8	25.8±5.0	0.86
<b><i>Clinical characteristics</i></b>			
6M-WD (m)	382±112	290±108	<b>&lt;0.01</b>
Log NT-ProBNP	2.83[1.07]	3.44[0.95]	<b>&lt;0.01</b>
<b><i>Right heart catheterization</i></b>			
PAP (mmHg)	46±15	43±12	0.24
PVR (dynes*s/cm <sup>5</sup> )	652±493	658±329	0.95
CO (l/min)	4.8±1.3	4.7±1.9	0.84
CI (l/min/m <sup>2</sup> )	2.7±0.8	2.5±1.0	0.37
<b><i>Echocardiography</i></b>			
RVEDA (cm <sup>2</sup> )	28±7	32±9	<b>&lt;0.01</b>
RVESA (cm <sup>2</sup> )	18±6	23±8	<b>&lt;0.01</b>
RVFAC (%)	35±7	31±10	<b>&lt;0.01</b>
TAPSE (cm)	2.0±0.4	1.8±0.4	0.06
RA area (cm <sup>2</sup> )	21±7	22±6	0.29
<b><i>ε-area loop</i></b>			
ESslope	-1.3±1.0	-1.1±1.0	0.23
Sslope (%/cm <sup>2</sup> )	-1.9±0.8	-1.5±0.6	<b>&lt;0.01</b>
Peak ε (%)	-16.3±4.5	-14.0±4.7	<b>&lt;0.01</b>
UNCOUP_ED (AU)	2.0±2.4	1.7±2.1	0.47
UNCOUP_LD (AU)	2.0±2.4	1.8±2.1	0.68
UNCOUP(AU)	2.0±2.3	1.7±2.0	0.52
EDslope (%/cm <sup>2</sup> )	1.3±1.1	1.0±0.8	0.25
LDslope (%/cm <sup>2</sup> )	2.2±1.2	1.8±0.9	<b>0.02</b>

432 BSA=Body Surface Area; BMI=Body Mass Index; PAP=Pulmonary Arterial Pressure;  
 433 PVR=Pulmonary Vascular Resistance; CO=Cardiac output; CI=Cardiac Index; 6M-WD=6  
 434 Minute Walking Distance; RVEDA=Right ventricular end diastolic Area; RVESA=Right  
 435 ventricular end systolic area; RVFAC=Right ventricular fractional area change;  
 436 TAPSE=Tricuspid annular plane systolic excursion.

437 **TABLE 3** - Univariate cox-regression hazard ratio's of currently used predictors and  
 438 echocardiographic derives indices of RV structure and function including the RV  $\epsilon$ -area loop  
 439 characteristics.

	<i>Univariate HR [95%- CI]</i>	<i>p-value</i>
Age (y)	1.023 [1.002-1.044]	<b>0.03</b>
Sex (Male)	2.191 [1.210-3.968]	<b>0.01</b>
NT-ProBNP (>1400 ng/l)	3.215 [1.727-5.982]	<b>&lt;0.01</b>
6M-WD (<165 m)	2.873 [1.005-8.209]	<b>&lt;0.01</b>
RA Area (>26 cm <sup>2</sup> )	1.310 [0.676-2.537]	0.42
RVEDA (>26.8 cm <sup>2</sup> )	2.777 [1.405-5.488]	<b>&lt;0.01</b>
RVESA (>16.9 cm <sup>2</sup> )	3.690 [1.775-7.669]	<b>&lt;0.01</b>
RVFAC (<25.5 %)	5.429 [2.973-9.914]	<b>&lt;0.01</b>
TAPSE (<1.95 cm)	2.199 [1.202-4.022]	<b>0.01</b>
ESslope (>-1.695 %/cm)	2.658 [1.125-6.282]	<b>0.03</b>
Sslope (>-1.62 %/cm)	2.124 [1.161-3.886]	<b>0.01</b>
Peak $\epsilon$ (>-14.45 %)	3.400 [1.858-6.222]	<b>&lt;0.01</b>
UNCOUP_ED (<1.025)	1.840 [1.025-3.301]	<b>0.04</b>
UNCOUP_LD (<2.035)	1.362 [0.745-2.491]	0.32
UNCOUP (<0.805)	1.557 [0.861-2.813]	0.14
EDslope (<0.95 %/cm)	1.800 [1.000-3.238]	<b>0.05</b>
LDslope (<2.465 %/cm)	2.684 [1.198-6.014]	<b>0.02</b>

440 Abbreviations are explained below Table 2.

441

442 **TABLE 4** – Independent predictive value for 5-years survival of echocardiographic derived  
 443 parameters within a multivariable model, including, age, sex 6MWD and log NT-proBNP as  
 444 baseline model.

	<b>60 [45-60] months 45 events</b>	
	<i>HR [95%-CI]</i>	<i>p-value</i>
RVEDA (cm <sup>2</sup> )	1.566 [0.670-3.656]	0.30
RVESA (cm <sup>2</sup> )	2.520 [1.014-6.265]	<b>0.05</b>
RVFAC (%)	3.671 [1.635-8.238]	<b>&lt;0.01</b>
TAPSE (cm)	1.322 [0.641-2.728]	0.45
ESslope (%/cm)	1.865 [0.707-4.924]	0.21
Sslope (%/cm)	1.089 [0.491-2.415]	0.84
Peak strain (%)	2.597 [1.135-5.943]	<b>0.02</b>
UNCOUP_ED (AU)	1.325 [0.662-2.653]	0.43
EDslope (%/cm)	1.347 [0.647-2.802]	0.43
LDslope (%/cm)	1.776 [0.711-4.435]	0.22

445 Abbreviations are explained below Table 2.

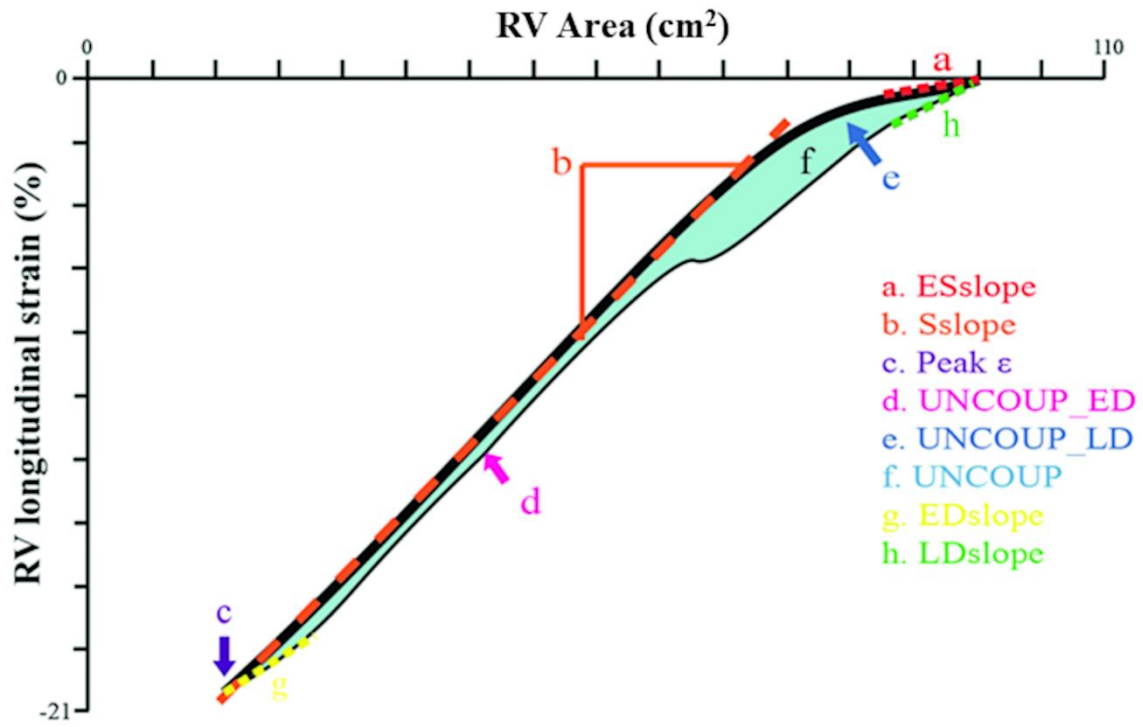
446

447 **FIGURE LEGENDS**

448 **FIGURE 1** – Schematic overview of the RV  $\epsilon$ -area loop and the derived characteristics. The

449 black line represents the  $\epsilon$ -area loop, the thick part represents the systolic phase and

450 the thin line the diastolic phase.

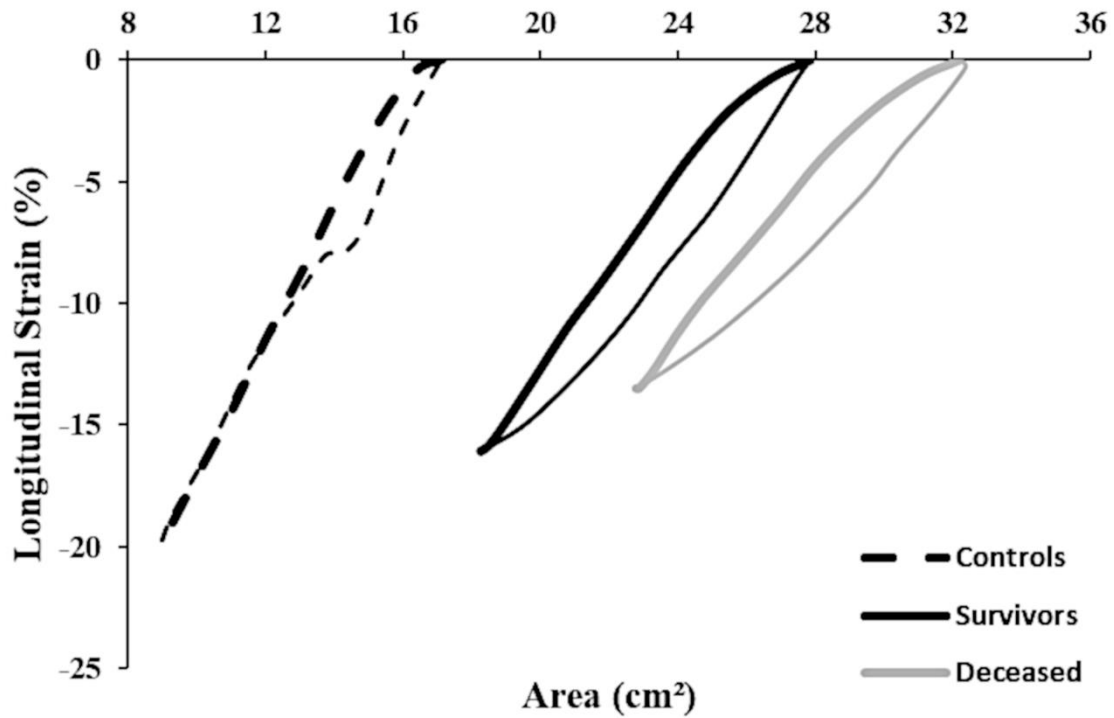


451

452

453

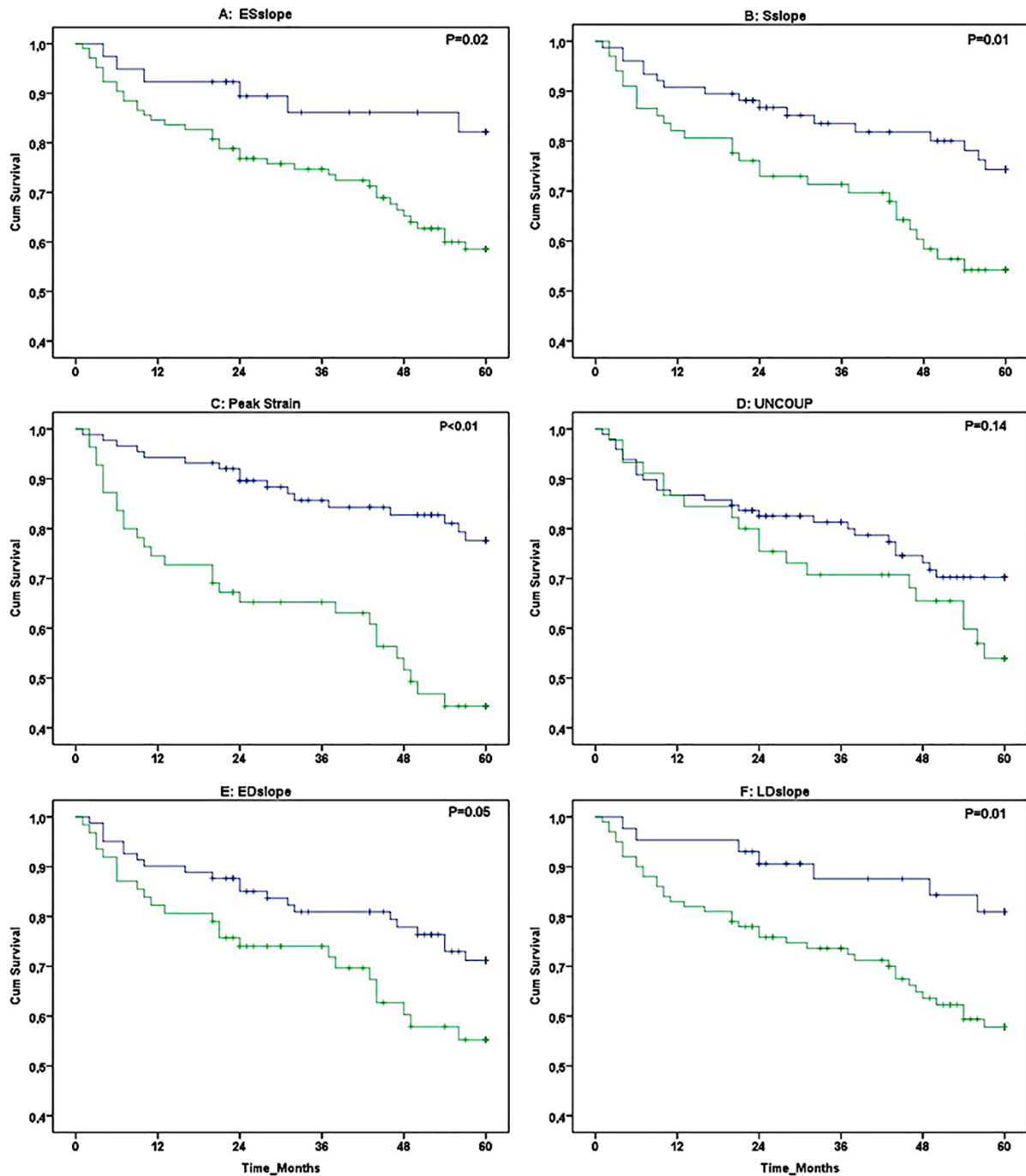
454 **FIGURE 2** – Mean RV  $\epsilon$ -area loops taken at baseline (i.e. start of the follow-up period) from  
455 surviving patients (black  $\epsilon$ -area loop, n=98) and deceased patients (grey  $\epsilon$ -area loop,  
456 n=45). The dotted black lines represent the  $\epsilon$ -area loop in a control group as published  
457 previously.(8) The thick lines represents the systolic phase while the thin lines  
458 represent the diastolic phase of the  $\epsilon$ -area loop.



459  
460



461 **Figure 3** – Kaplan-Meier survival curves (5-yr follow-up) in 143 PH patients for individual  
462 characteristics of the RV  $\epsilon$ -area loop that were categorised into low risk (blue line)  
463 and high risk (green line). The following loop characteristics were presented:  
464 ESslope (A), Sslope (B), peak strain (C), Uncoup (D), EDslope (E) and LDslope (F).



465

466

467 **Figure 4** – Kaplan-Meier survival curves for A) the RV loop-score, categorised into low risk  
 468 (blue line, n=98) versus high risk (green line, n=45), B) the 2015 ESC/ERS  
 469 guidelines based model, categorised into low (blue line, n=23), intermediate (green  
 470 line, n=60) and high risk (red line, n=39) and C) the combined RV loop-score and  
 471 ESC/ERS based model, categorised into low risk (blue line, n=23), intermediate risk  
 472 (green line, n=60), high risk – low RV loop-score (orange line, n=20) and high risk  
 473 – high RV loop-score (purple line, n=19).

